

## RESEARCH ARTICLE

# Apoptotic Effects of Eugenol-loaded Nanoemulsions in Human Colon and Liver Cancer Cell Lines

Hamid Majeed, John Antoniou, Zhong Fang\*

### Abstract

**Background:** In this study eugenol (EU) loaded nanoemulsions (NEs) emulsified with modified starch were prepared and their apoptotic potential against liver and colon cancer cells was examined in comparison with bulk EU. **Materials and Methods:** We prepared stable EU loaded NEs which were characterized by dynamic light scattering, centrifugation and gas chromatography. Furthermore, cell viability was determined using MTT assay, and apoptosis and cell cycle analyses by flow cytometry. **Results:** HB8065 (liver) and HTB37 (colon) cells when treated with EU:CA NEs demonstrated greater apoptotic cells percentages as evidenced by microscopic images and flow cytometric evaluations. It was observed that EU and EU:CA NE induced apoptosis in both cell lines via reactive oxygen species (ROS) generation. **Conclusions:** The present study demonstrated that ROS plays a critical role in EU and EU:CA NE induced apoptosis in HB8065 and HTB37 cells. This is the first report on the antiproliferative mechanisms of EU loaded NE.

**Keywords:** Reactive oxygen species - liver - colon cell line - eugenol - eugenol nanoemulsion

*Asian Pac J Cancer Prev*, 15 (21), 9159-9164

### Introduction

Colon cancer is the third most common cancer of western countries and its percentage is increasing every year (Hagggar and Boushey, 2009). Liver cancer is the fifth most common diagnosed cancer type in males but second leading cause of death in developing countries (Jemal et al., 2009). To prevent such degenerative diseases, natural and synthetic drugs have gained significant attention. Unfortunately, synthetic drug based strategies are expensive and may have side effects, such as decreased pathogen sensitivity due to multiple uses.

EU is a natural phytochemical found in cloves (*Syzygium aromaticum* L.) and has analgesic, antibacterial, antiinflammatory and anticancerous properties (Zheng et al., 1992; Moon et al., 2011). It has been often used in medical practices in Asia. EU has been reported to inhibit colon cancer cell proliferation by arresting the cells in sub G1 phase, augment ROS levels that result in DNA fragmentation, which is a hallmark of apoptosis. It has been reported that EU is a phenolic compound that induces apoptosis in human colon cancer cells (Jaganathan et al., 2011). Similarly, alleviated ROS levels also induced apoptosis in human promyelotic leukemia cells (HL60) when exposed to EU (Yoo et al., 2005). kim et al., (2003) reported inhibition of cyclooxygenase2 (COX2) gene responsible for colon cancer cell proliferation when HT-29 (colon cancer cell line) was treated with EU. Cytotoxicity of EU against hepatoma carcinoma cell line (HEPG2) resulted in decreased glutathione levels (Babich

et al., 1993). The antiproliferative activity of EU against melanoma (Ghosh et al., 2005), leukemia (Jaganathan et al., 2011), gastric (Benencia and Courreges, 2000), skin tumor (Chogo and Crank, 1981) and prostate cancer (Asha et al., 2001) cells has been confirmed by many researchers.

Polyphenols like EU have been found to have low solubility in water. This results in low bioavailability when administered orally due to its limited solubility. To enhance availability of antitumor drugs like EU and curcumin nanotechnology based strategies could be advantageous. NE have been used to increase the bioavailability of polyphenols. For example, curcumin was mixed with MCT (medium chain triglyceride), SCT (short chain triglyceride) and LCT (long chain triglyceride oil) to prepare a lipid phase which was emulsified with  $\beta$ -lactoglobulin solution to prepare a NE. NE having particle size of 174 nm showed maximum curcumin bioaccessibility (Ahmed et al., 2012). Similarly Terjung et al. (2012), prepared EU loaded NEs using EU and MCT as a lipid phase and reported its enhanced bioavailability in aqueous phase due to solubility in surfactant micelles. They also confirmed enhanced bactericidal action of EU NEs. Chen et al. (2011) reported apoptotic activity of curcumin loaded NEs against colon cancer cell lines with an IC50 value of 24.66 and 24.02  $\mu$ m. Apoptosis is a self destructive cell death mechanism involving nuclear condensation, cytoplasmic organelles and formation of apoptotic bodies (Srivastava et al., 2007). Only the bactericidal action of EU loaded NEs has been documented but no one has reported its anticancerous

potential. In this study we prepared EU loaded NEs and evaluated their anti-proliferative mechanism against liver (HEPG2) and colorectal cancer (Caco2) cell lines.

## Materials and Methods

### Materials

Eugenol (EU; Product E10439, Canspec, Shanghai, China), MCT (Neobee-1053, NHG-DMEM, RPMI (Gibco BRL, Life Technologies, USA), Trypsin-EDTA solution (Beyotime, Jiangsu, China), fetal bovine serum (FBS; Sijiqing, Zhejiang, China), Annexin V/FITC kit (Beyotime, Jiangsu, China), Hoechst33258 kit (Beyotime, Jiangsu, China), Cell cycle and ROS assay kit (Beyotime, Jiangsu, China), MTT and Propidium iodide (Sigma, St. Louis, MO, USA), SH-1000 Lab microplate reader (Corona Electric Co. Ltd., Ibaragi, Japan), SpectraMax M5 Multifunctional microplate reader (Molecular Devices, USA), Olympus BX41 fluorescent microscope (Olympus, Tokyo, Japan) and FACS Calibur flow cytometer (BD Co., USA).

### Preparation of nanoemulsion

EU loaded NEs were prepared by using the same procedure as described in our previous study (manuscript submitted). Briefly, a 10% (v/v) lipid phase of a medium chain triglyceride (MCT) and canola oil (CA), EU: MCT, and EU: CA in variable ratios were emulsified with 2% wt/wt purity gum ultra (PGU) solution to prepare coarse emulsion and then passed through a high pressure homogenizer at 150 Mpa pressure, 5 processing cycles (Table: 1).

### Particle size measurement

Emulsion particle size were measured by dynamic light scattering and phase analysis light scattering (Zetasizer Nano ZS, Malvern Instruments, Malvern, U.K.), using 1 mL emulsion samples diluted 100x with deionized water to avoid multiple light scattering effects. For dynamic light scattering, the particle size data are reported as Z-average mean diameter and polydispersity index (PDI).

### Stability of emulsion

NEs developed by high pressure homogenization were centrifuged at 10,000g for 30 min, and the stability of formulated NE to centrifugation was studied. Kinetic stability was determined in terms of droplet diameter at different interval of time (1, 15 and 30 days) using particle size analyzer.

### Extraction and determination of EU in nanoemulsions

EU was extracted from emulsions using dichloromethane (Donsi et al., 2011) and quantitated by GC. Briefly, 4ml of dichloromethane was added to 2ml of NE, followed by three vortex agitations of 10 second each. The organic phase was recovered with pasteur pipette and anhydrous sodium sulphate was added to remove residual water. The EU extract was micro-filtered and placed for 15 minutes under nitrogen flow in order to completely evaporate the solvent. 2  $\mu$ l of the resulting EU extract were added to n-hexane and analyzed by

GC. To determine the content of EU in emulsion, GC analyses were performed using a Shimadzu GC- 2010 gas chromatograph equipped with HP-INNOWAX capillary column (0.30m $\times$ 0.32mm $\times$ 0.25 $\mu$ m) and a flame ionization detector (FID). Oven temperature was 40°C for 2 min and then programmed heating from 40 to 100°C at a rate of 8°C /min, and at 230°C at the rate of 10°C/min.

### Cell culture

Liver HepG2 (ATCC-HB8065) and Colon cancer (ATCC-HTB37) cells were obtained from American Type Culture Collection and used according to their recommendations. Briefly, Cells were maintained in DMEM and RPMI 1640 supplemented with 10% FBS, 100  $\mu$ g/ml penicillin and 100  $\mu$ g/ml streptomycin incubated with 5% CO<sub>2</sub> at 37°C. Both cell types were treated with various concentrations of EU and EU NE for 24 h.

### Cell viability assay

Cell survival was determined by the reduction of MTT to formazan crystals by mitochondrial dehydrogenases. Briefly, cells were seeded at a density of 2 $\times$ 10<sup>3</sup> cells/mL in a 96-well plate, after 12 h of cell attachment, cells were treated with EU or EU NEs (50- 1500  $\mu$ M) and incubated for 24 h. Next, 20  $\mu$ L of MTT solution (5 mg/ml in PBS) was added to each well and the cells further incubated at 37°C for 4 h in a 5% CO<sub>2</sub> humidified incubator. The medium was carefully removed, and colored formazan were dissolved in 150  $\mu$ L dimethyl sulfoxide (DMSO). The plate was shaken for 10 min and the absorbance was measured at 490 nm or 570 nm using a microplate reader (SPECTRA FLUOR). Cell viability was expressed as percent of the control culture value.

### Assessment of cell morphology

HB8065 and HTB37 cells were observed with a fluorescence microscope (Olympus Optical Co. Ltd., Japan) after staining with Hoechst33258 dye. Cells were seeded into 6-well plates. After various treatments, cells were fixed for 30 min with 4% paraformaldehyde at room temperature. Then cells were washed and stained with Hoechst33258 (10  $\mu$ g/mL) for 10 min in a 5% CO<sub>2</sub> humidified incubator. Finally, cells were observed under converted fluorescence microscope, and images were recorded with a CCD.

### Apoptosis/Necrosis Assay with Flow Cytometry Analysis

cells were seeded at 5 $\times$ 10<sup>4</sup> cells per well in six-well plate with the same conditions as described above in the MTT assay and cell apoptosis was detected by annexin V-FITC apoptosis detection kit following manufacturer's instructions. Briefly, the cells were gently trypsinized, washed with PBS, re-suspended in binding buffer and incubated with annexin V-FITC and PI at room temperature in the dark for 10 min, and analyzed immediately by FACScan Flow Cytometer (Beckman coulter, Epics).

### Measurement of reactive oxygen species (ROS)

2',7'-dichloro-fluorescein diacetate (DCFH-DA) is a fluorescent probe, transported across the cell

membrane and hydrolyzed by intracellular esterases to form nonfluorescent 2',7'-dichloro fluorescein (DCFH), which is finally converted to highly fluorescent 2',7'-dichlorofluorescein (DCF) in the presence of reactive oxygen species (ROS). The DCF fluorescence intensity is believed to parallel the amount of ROS formed intracellular. To determine the amounts of ROS induced by EU and EU:CA NE, DCFH-DA (50  $\mu$ M DMSO) was added to the cells culture and then incubated at 37°C for 20 min. The production of ROS was measured immediately with a microplate reader using excitation and emission at 485 nm and 530 nm, respectively.

## Results

### Preparation of nanoemulsions

Ostwald ripening inhibitors (MCT and LCT) have been used by many researchers to prepare stable NEs for a longer time period (Kabalnov, 2001). Therefore, in our study we blended EU with MCT and CA in different ratios and the droplet size distributions of emulsions containing different concentrations of EU:CA, EU:MCT when prepared at 150 MPa pressure with 5 processing cycles and 2% wt/wt PGU are shown in Table: 1. The droplet size decreased from 227 -153 nm and 222-150 nm in EU:CA and EU:MCT formulations. It was observed that with increase of EU percentage, the droplet diameter and PDI decreases. Surprisingly, at concentrations above EU ratio i.e, 5:5% v/v, both emulsion formulations (EU:MCT & EU:CA) showed increase in droplet diameter distributions at the same homogenization pressure and processing cycles. Terjung et al., (2012) observed similar effects of polyphenols and oil emulsions. They observed that critical limits for EU and carvacol were 50 and 30% wt/wt in oil phase respectively. Above critical limit the emulsions (> 50% w/w) separated into a cream layer and serum layer after standing for several hours despite the smaller initial droplet sizes. The particles in the cream layer grew larger without flocculation but no coalescence in emulsions with lower EU content was observed. Therefore, the loading of emulsion with EU is limited by the amount and solubility properties of the other lipid phase. So, we decided to use 5:5% (v/v) EU:MCT and EU:CA NE, because of smaller particle size among all formulations.

### Effect of storage time on droplet diameter and stability

The mean droplet diameters of all emulsion formulations increased with the storage time. Both EU:MCT and EU:CA NEs showed almost 20-30 nm increase in the droplet diameter (data not shown). This

increase in droplet diameter was observed in case of peppermint oil NE formulations (Liang et al., 2012). On the other hand no phase separation was observed. All the formulated emulsions were stable after centrifugation at 10,000 rpm for 30 minutes.

### Extraction and determination of EU in nanoemulsions

EU is highly susceptible to oxygen, light or heat and gas chromatography was used to quantitate the EU in emulsion. In order to confirm the oxidative stability of EU in NE, both 5:5% (v/v) EU:MCT and EU:CA formulations were analyzed. The EU content in both formulations was 99.51 and 99.45%, compared with the original loading concentration.

### Antiproliferative effect of EU and EU loaded nanoemulsions

MTT assay was used to assess the antiproliferative effect of EU and EU NEs against liver (HB-8065) and colon cancer cells (HTB-37). Cells were treated with different concentrations of EU and EU NEs (0-1500  $\mu$ M) for 24 hours. Their inhibitory effects against HB-8065 and HTB-37 are shown in Figure 1, respectively. Growth inhibition of cells in case of both EU and EU NEs was dependent on dose and cell line type used. Both HB-8065 and HTB-37 were repressed significantly with an IC50 value of 500 and 750  $\mu$ M of bulk EU, respectively.

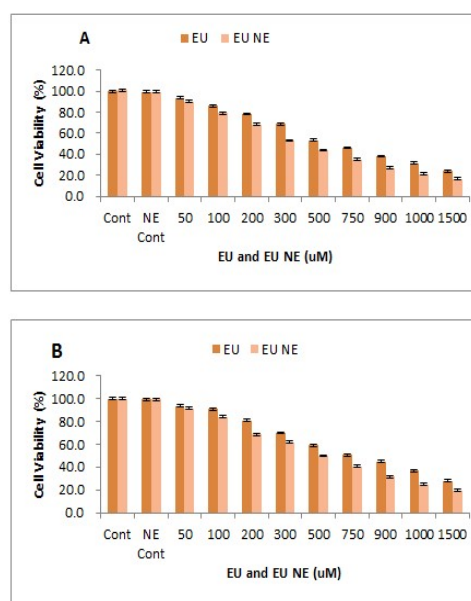


**Figure 1. Antiproliferative Effect of EU and EU:CA NE against HB8065 (A) and HTB37 (B) Cells.** EU: Eugenol; NE: Nanoemulsion; Cont: Control; NE Cont: Nanoemulsion Control

**Table 1. Emulsion Formulations, Corresponding Particle Sizes and Polydispersity Index (PDI) of Nanoemulsions Prepared using 2% wt/wt PGU, 150 MPa Pressure and 5 Processing Cycles**

Emulsion Formulation (V/V %)	EU: CA		EU: MCT	
	Particle Size(nm)	PDI	Particle Size(nm)	PDI
10:0% (CA &MCT)	227.67±3.742	0.21±0.008	222.33±5.073	0.21±0.008
1:9 %	205.27±0.188	0.21±0.001	203.07±0.047	0.26±0.001
3:7 %	196.43±1.887	0.20±0.006	194.13±1.562	0.19±0.020
5:5 %	153.40±1.766	0.15±0.036	150.10±1.557	0.13±0.034
7:3 %	248.53±0.377	0.32±0.001	241.27±0.895	0.22±0.002

\*CA:canola oil, EU: Eugenol, MCT: Medium chain triglyceride oil

Whereas, for EU NEs IC50 values reduced to 300 and 500  $\mu$ M for HB-8065 and HTB-37. Both EU:MCT and EU:CA showed similar IC50 values against both cell lines (Data not shown for EU:MCT). Therefore, we decided to use EU:CA NE for further experiments. Moreover, we observed that HB-8065 cells were more sensitive to EU and EU:CA NE than HTB-37 cells. The MTT assay suggested significant antiproliferative effect of EU and EU:CA NE against HB-8065 cells. Eugenol and Eugenol nanoemulsion induced cell morphological changes

Incubation of HB-8065 & HTB-37 cells with EU and EU:CA NE resulted in shrinkage of the cell nucleus and condensed chromatin material adjacent to the plasma membrane. The nucleus broke into small fragments and cellular debris extruded out via budding from the plasma membrane and formed apoptotic bodies (Figure 2).

*Eugenol and Eugenol nanoemulsion induced damage in HB8065 and HTB37 cells*

Propidium iodide (PI) is membrane impermeant has entered the damaged cells and used for the detection of apoptotic or damaged cells during flow cytometry. HTB-37

cells when exposed to EU and EU:CA NE showed 51 and 57% apoptotic cells, respectively Figure: 3A3 and 3A4. On the other hand, HB8065 cells when exposed to EU and EU:CA NE resulted in significantly higher apoptosis percentages i.e., 53 and 69% respectively, Figure: 5B3 and 5B4. These results confirmed more sensitivity of EU and EU:CA NE against HB8065 as cells compared to HTB 37. These findings suggest that cytotoxicity of EU and EU:CA NE against HB-8065 and HTB-37 cells is caused by the induction of apoptosis. EU induced apoptosis by mitochondrial pathway in gastric carcinogenic cells as evidenced by the findings of (Manikandan et al., 2010).

*Eugenol and Eugenol loaded nanoemulsions induced cell cycle arrest*

HB8065 and HTB37 cells were treated with EU & EU:CA NE and cell cycle analysis was performed using flow cytometry. In control HB8065 cells, the distribution of cells in G1, S and G2 phases of cell cycle were 51 %, 40 % and 8 %, respectively. Treatment of HB8065 cells with EU resulted in increased number of cells in sub G1 & S phases with concomitant reduction of cell number in G1

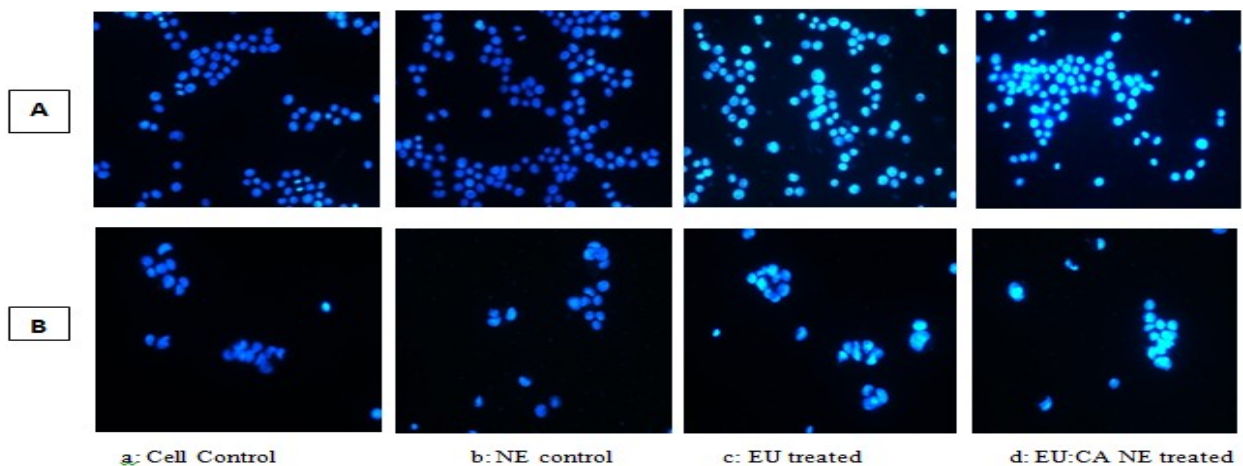


Figure 2. Morphological analysis of HB8065 (A) and HTB37 (B) Cells by Hoechst 33258 (DNA Fluorescent Dye) Staining

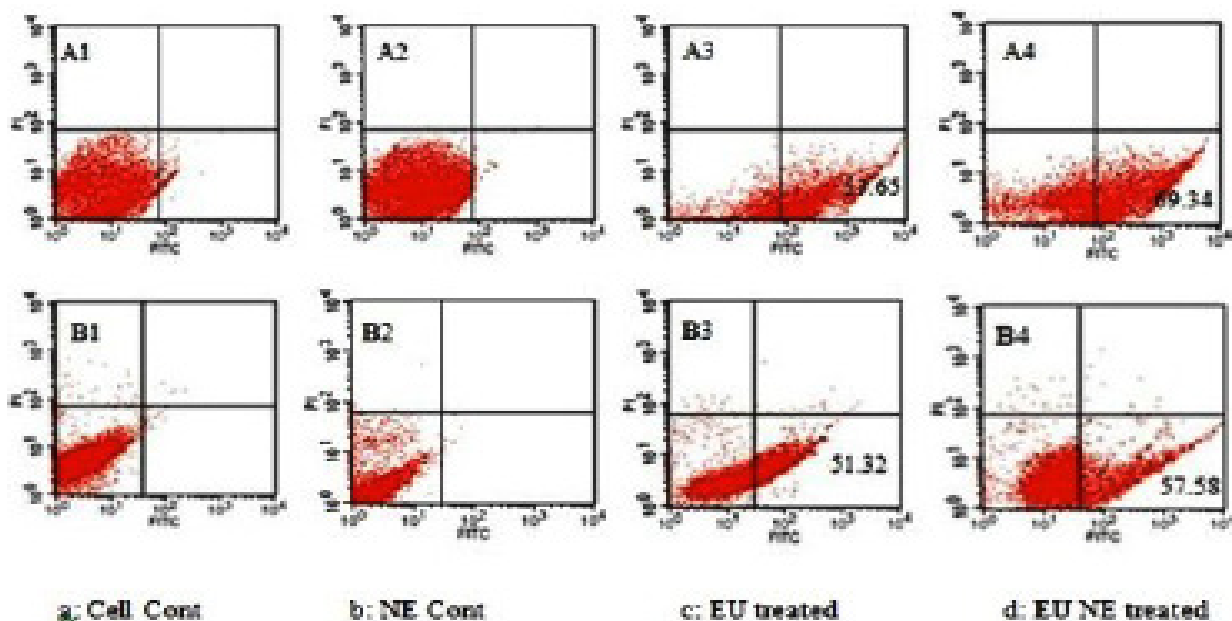


Figure 3. Images of EU and EU NE induced Apoptosis of HB8065 (A) and HTB37 (B) Cells

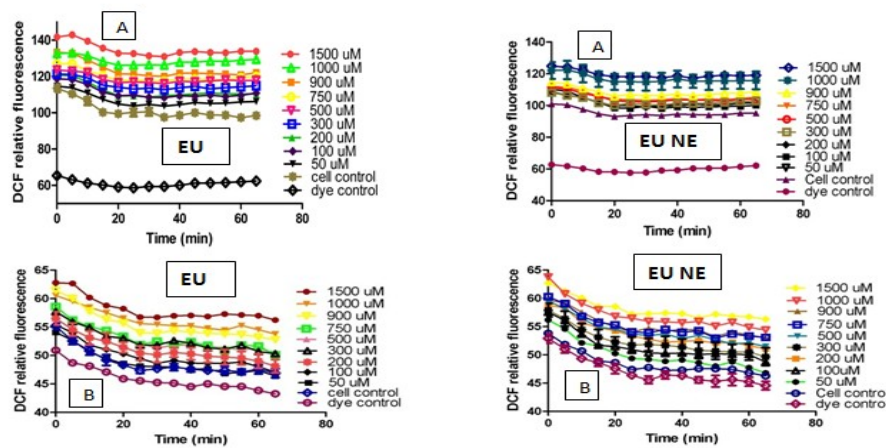


Figure 4. EU, EU: CA NE Induced Intracellular ROS Levels in HB8065 (A) and HTB37 (B) Cells

Table 2. Percentage Distribution of HB8065 and HTB37 Cells After EU and EU-CA NE Treatments among Various Cell Cycle Stages

	Sub-G1	G0/G1	S	G2/M
<b>HB8065</b>				
Control	0.77±0.01	50.41±0.61	40.11±0.08	8.44±0.03
NE Control	1.08±0.02	41.34±0.01	50.35±0.1	8.14±0.01
EU control	25.50±0.008	60.10±0.3	36.10±0.03	3.30±0.009
EU:CA NE	32.12±0.01	31.01±0.009	67.04±0.04	1.92±0.004
<b>HTB37</b>				
Control	0.09±0.004	51.30±0.01	38.84±0.1	12.50±0.01
NE Control	0.52±0.02	48.60±0.4	39.09±0.02	12.47±0.06
EU control	15.20±0.01	50.90±0.4	45.53±0.1	4.21±0.07
EU:CA NE	19.40±0.2	37.12±0.06	61.70±0.04	1.23±0.02

\*CA:canola oil, EU: Eugenol, NE: Nanoemulsion

(51.30-36.16%) and G2 (8.49-3.31%) phases. However, in case of EU NE treated cells, cells arrested in sub G1 & S phase increased significantly (1.11- 32.13%, 41.35 - 67.04% respectively). EU and EU:CA NE induced cell cycle arrest at sub G1/S phase in both cell lines as shown in Table 2.

#### ROS generation:

ROS generation after EU and EU:CA NE treatments were investigated using ROS-sensitive probe DCF in HB8065 and HTB37 cells. ROS levels elevated significantly in the case of both HB8065 & HTB37 cells when treated with EU and EU:CA NE. In the case of HB8065 cells when treated with EU the fluorescence intensity increased from 120 to 140 as compared to the control, Figure.4A. Whereas, fluorescent intensity increased from 100 to 125 in case of EU:CA NE treated cells. On the other hand, HTB37 cells showed increased DCF fluorescence intensity from 55-63, 53-65, respectively when treated with EU and EU:CA NE (Figure 4B).

## Discussion

Stable nanoemulsion preparations resistant to coalescence and Ostwald ripening have been studied by many researchers (Terjung et al., 2012; Liang et al., 2012). For example D-limonene was blended with palm oil (1:1) to increase the stability of NE against physical factors like coalescence and Ostwald ripening. Similarly, EU, peppermint oil, D-limonene and cinnamaldehyde based

NE have already been prepared by mixing with MCT (Neobee 1053, Miglyol 812N) and LCT (Corn, soybean oil) for improved stability. In addition to the stability, size of NEs is a prime factor that determines the biological activity of entrapped bioactive compound. Recent studies have shown that NE with small droplet size increases the bioavailability of encapsulated lipophilic compounds (Wang et al., 2008; Acosta, 2009; Qian and McClements, 2011). Curcumin oil in water NE showed significant reduction in cancer cells growth with decreasing emulsion droplet diameter (Wang et al., 2008). Similarly, curcumin encapsulated in liposomes having particle size 100-150 nm also showed increased anticarcinogenic potential against human prostate cancer cells (Thangapazam et al., 2008). Furthermore, encapsulated curcumin having size 100 nm was more accessible to cancer cells and inhibitory concentration reduced to 14.34  $\mu$ m (Das et al., 2010). In our case EU NEs showed lower inhibitory concentration values against both HB8065 and HTB37 cell lines compared to EU alone. The IC50 values obtained in our study were in accordance to the findings of (Babich et al., 1993; Jaganathan et al., 2011). These findings strengthen the previous researches that essential oils or their constituents when incorporated in smaller NEs increased their accessibility and ultimately resulted in their enhanced bioactivity. The visual observation of cells after EU:CA NE treatment showed maximum apoptotic cell demise (cell shrinkage, chromatin condensation and internucleosomal cleavage of genomic DNA) that has been confirmed by other researchers (William, 1991). The same apoptotic phenomenon was observed by (Pisano et al., 2007; Dwivedi et al., 2011) when cervical, prostate, breast, prostate and oesophageal cancer cell lines were treated with clove oil extract. However, flow cytometric observation further confirmed pronounced apoptotic potential of EU:CA NE in both cell lines HB8065 and HTB37 at lower IC50 values compared to EU alone. Similarly, in case of HTB37 cells, EU and EU:CA NE induced growth arrest at sub G1/S phases of cell cycle. These results were in accordance to the findings of (Jaganathan et al., 2011), who reported Sub G1 cell cycle arrest in colon cancer cell lines (HCT-15 & HT-29) when treated with EU. These findings further strengthened by the findings of (Yang et al., 2000; Srivastava et al., 2007). Tan et al., (2006) reported sub G0/G1 cell cycle arrest in HL-60 cells when treated with 1

uM curcumin. These results confirmed similar mechanism of cell cycle growth arrest of both EU and EU:CA NE.

On the other hand, ROS generation is an important phenomenon in the apoptosis induced by anticancer agents (Jaganathan et al., 2011; Simbula et al., 2007). Yoo et al., (2005) reported ROS generation in HL-60 cells when treated with EU. HL-60 cells showed increased level of ROS after incubation with 1 uM curcumin at different time intervals. The cells showed increase in ROS levels from (1.4±0.6 - 74.8±6.7) when incubated from 15 to 240 minutes time period (Tan et al., 2006). Simbula et al., (2007) also found increase in ROS levels when hepatoma cell lines (Fao) and HepG2 were treated with alpha lipoic acid. We observed similar phenomenon of elevated ROS levels when both cell lines were treated with EU and EU:CA NE.

EU:CA NE showed an antiproliferative effect against colon and liver cancer cell lines depending upon the concentration and the cell lines used. Further, EU:CA NE exhibited lower IC50 values against both cell lines compared to EU. Both EU and EU:CA NE induced sub G1/S cell cycle arrest and apoptosis via ROS dependent mechanism. Thus our results suggest that EU and EU:CA NE have similar antiproliferative mechanisms against both cell lines. Therefore, our research further enhances EU as a potential chemopreventive agent against liver and colon cancer. In future precise mechanism of intracellular induced ROS that triggers apoptosis will be considered.

## Acknowledgements

This work was financially supported by National 863 Program 2011BAD23B02, 2013AA102207, NSFC 31171686, 30901000, 111 project-B07029 and PCSIRT0627.

## References

Acosta E (2009). Bioavailability of nanoparticles in nutrient and nutraceutical delivery. *Curr Opin Colloid Interface Sci*, **14**, 3-15.

Ahmed K, Li Y, McClements DJ (2012). Nanoemulsion and emulsion based delivery systems for curcumin: Encapsulation and release properties. *Food Chem*, **132**, 799-807.

Asha MK, Prashanth D, Murali B (2001). Anthelmintic activity of essential oil of *Ocimum sanctum* and eugenol. *Fitoterapia*, **72**, 669-70.

Babich H, Stern A, Borefreund E (1993). Eugenol cytotoxicity evaluated with continuous cell lines. *Toxicol Vitro*, **7**, 105-9.

Benencia F, Courreges MC (2000). *In vitro* and *in vivo* activity of eugenol on human herpesvirus. *Phytother Res*, **14**, 495-500.

Chen M, Chu Y, Lai P (2011). Experimental results of colorectal cancer chemoprevention by curcuminoids loaded nanocarrier drug delivery system increased *in vitro* biocompatibility. *Dig J Nanomater Biostruct*, **6**, 1187-97.

Chogo JB, Crank G (1981). Chemical composition and biological activity of the tanzanian plant *Ocimum suave*. *J Nat Prod*, **42**, 308-11.

Das RK, Kasaju N, Bora U (2010). Encapsulation of curcumin in alginate-chitosan-pluronic c composite nanoparticles for delivery to cancer cells. *Nanomedicine*, **6**, 153-60.

Donsi F, Annunziata M, Vincenzi M (2011). Design of nanoemulsion based delivery systems of natural

antimicrobials: Effect of the emulsifier. *J Biotechnol*, **159**, 324-50.

Dwivedi V, Shrivastava R, Hussain S (2011). Comparative anticancer potential of clove (*Syzygium aromaticum*) an Indian spice against cancer lines of various anatomical origin. *Asian Pac J Cancer Prev*, **12**, 1989-93.

Ghosh R, Nadiminty N, Fitzpatrick JE (2005). Eugenol causes melanoma growth suppression through inhibition of E2F1 transcriptional activity. *J Biol Chem*, **280**, 5812-9.

Haggar FA, Boushey RP (2009). Colorectal cancer epidemiology: incidence, mortality, survival and risk factors. *Clin Colon Rectal Surg*, **22**, 191-97.

Jaganathan SK, Mazumdar A, Mondhe D (2011). Apoptotic effect of eugenol in human colon cancer cell lines. *Cell Biol Int*, **35**, 607-15.

Jemal A, Siegel R, Ward E (2009). Global cancer statistics. *CA: A Cancer J Clin*, **59**, 225-49.

Kabalnov A (2001). Ostwald ripening and related phenomena. *J Dispersion Sci Technol*, **22**, 1-12.

Kim SS, Oh OJ, Min HY (2003). Eugenol suppresses cyclooxygenase-2 expression in lipopolysaccharide-stimulated mouse macrophage RAW264.7 cells. *Life Sci*, **73**, 337-48.

Liang R, Xu S, Shoemaker CF (2012). Physical and antimicrobial properties of peppermint oil nanoemulsions. *J Agric Food Chem*, **60**, 7548-55.

Manikandan P, Murugan RS, Priyadarsini RV (2010). Eugenol induces apoptosis and inhibits invasion and angiogenesis in a rat model of gastric carcinogenesis induced by MNNG. *Life Sci*, **86**, 936-41.

Moon S, Kim H, Cha J (2011). Synergistic effect between clove oil and its major compounds and antibiotics against oral bacteria. *Arch Oral Biol*, **56**, 907-16.

Pisano M, Pagnan G, Loi M (2007). Antiproliferative and pro-apoptotic activity of eugenol related biphenyls on malignant melanoma cells. *Mol Cancer*, **18**, 6-8.

Qian C, McClements DJ (2011). Formation of nanoemulsions stabilized by model food-grade emulsifiers using high-pressure homogenization: Factors affecting particle size. *Food Hydrocolloids*, **25**, 1000-8.

Srivastava Rk, Chen Q, Siddiqui I (2007). Linkage of curcumin-induced cell cycle arrest and apoptosis by cyclin-dependent kinase inhibitor p21/WAF1/CIP1. *Cell Cycle*, **6**, 2953-61.

Tan T, Tsal H, Lu H (2006). Curcumin-induced cell cycle arrest and apoptosis in human acute promyelocytic leukemia HL-60 Cells via MMP changes and caspase-3 activation. *Anticancer Res*, **26**, 4361-72.

Terjung N, Loeffler M, Gibis M (2012). Influence of droplet size on the efficacy of oil-in-water emulsions loaded with phenolic antimicrobials. *Food Funct*, **3**, 290-301.

Thangapazham RL, Puri A, Tele S (2008). Evaluation of a nanotechnology-based carrier for delivery of curcumin in prostate cancer cells. *Int J Oncol*, **32**, 1119-23.

Wang XY, Wang YW, Jiang Y (2008). Enhancing bioavailability of curcumin through O/W nanoemulsions. *Food Chem*, **108**, 419-24.

William GT (1991). Programmed cell death. Apoptosis and oncogenesis. *Cell*, **65**, 1097-98.

Yang C, Shen H, Ong C (2000). Ebselen induces apoptosis in HepG2 cells through rapid depletion of intracellular thiols. *Arch Biochem Biophys*, **374**, 142-52.

Yoo CB, Han KT, Cho KS (2005). Eugenol isolated from the essential oil of *Eugenia caryophyllata* induces a reactive oxygen species-mediated apoptosis in HL-60 human promyelocytic leukemia cells. *Cancer Lett*, **225**, 41-52.

Zheng GQ, Kenney PM, Lam LKT (1992). Sesquiterpenes from clove (*Eugenia caryophyllata*). *J Nat Prod*, **55**, 999-1003.